Appl. Phys. B 57, 331–336 (1993)

Applied Physics B Photophysics and Laser Chemistry

Application of a Newly Developed CCD for Spectral-Width Measurements of a 53 eV Germanium Laser

H. Tsunemi[1], S. Nomoto[1], K. Hayashida[1], E. Miyata[1], H. Murakami[1], Y. Kato[2], G. Yuan[2], K. Murai[2], R. Kodama[2], H. Daido[2]

[1] Earth and Space Science, Faculty of Science, Osaka University, 1-1, Machikaneyama-cho, Toyonaka, Osaka 560, Japan
(Fax: +81-06/844-0509, Tel.: +81-06/844-1151, E-mail: tsunemi@oskar.kek.ac.jp)
[2] Institute of Laser Engineering, Osaka University, 2-6, Yamada-oka, Suita, Osaka 565, Japan
(Fax: +81-06/877-4799, Tel.: +81-06/877-5111)

Received 6 July 1993/Accepted 5 August 1993

Abstract. We report the application of a soft X-ray CCD for X-ray laser experiments. A newly developed CCD which has a thinned protection layer (SiO_2) of about 0.2 μm was attached to a grazing incidence spectrometer with a resolving power of 16000 in order to measure high-resolution spectra of a germanium soft X-ray laser. Clear spectra have been recorded with a high sensitivity in the energy range between 51 eV (240 Å) and 55 eV (225 Å). In addition to the two strong lasing lines at 236 Å and 232 Å, more than 20 weak spontaneous emission lines have been recorded in this energy range. The spectral width of the 236 Å lasing line is approximately 20.5 mÅ at the full width at half maximum. It is shown that this direct X-ray detection system has a spatial resolution of about 1/10 of the CCD pixel size in this spectral measurement.

PACS: 32.30.Rj, 42.55.Hq, 52.70.La

Remarkable progress has been made recently in the development of soft X-ray lasers covering the spectral range to 35.6 Å (350 eV) at the shortest wavelength [1, 2]. For the quantitative characterization of the soft X-ray lasers, reliable detectors that have high spatial resolution, high sensitivity, and a large dynamic range are necessary. Most X-ray detectors show poor detection efficiency in this low energy range. In previous X-ray laser experiments, X-ray films without overcoat emulsion layers or microchannel plates coupled to phosphor screens were used for recording two dimentional soft X-ray images. Charge-coupled devices (CCD) could become a better detector if it could be made very sensitive below ~1 keV, since CCDs in general have a low background, a large dynamic range, and a high spatial resolution, which is determined by fabrication technology. In this paper we report on the application of a CCD for high-resolution spectral measurement of the neon-like germanium soft X-ray laser at the photon energy of approximately 53 eV.

X-ray detectors can be divided into two categories. In the first category, which contains a gas-flow proportional counter, a solid-state detector and a microchannel plate, each X-ray photon is detected as a pulse signal. Since the photon energy is related to the signal pulse height, these detectors can have an energy resolving power when they are operated in the photon-counting mode. In the second category, which contains an X-ray film and an imaging plate, incident X-ray photons are integrated during one exposure time. Generally speaking, the latter detectors function as good X-ray imagers, but they have no energy resolving power since each photon is not counted as a single event.

Recently, a direct X-ray detection system using a charge-coupled device (CCD) has been developed. The CCD intrinsically belongs to the second category. The major advantage of this system, however, is that it can have a spatial resolution as well as an energy resolution for a moderate incident X-ray flux [3]. When the incident flux is not so large that each pixel detects at most one photon during its exposure time, the integrated charge in each pixel represents the energy of the individual X-ray photon. When the incident X-ray flux is larger and each pixel detects more than two photons, energy resolution is lost but the CCD still works well as a good X-ray imager having a large dynamic range with excellent linearity. The spatial resolution is determined by the pixel size which is typically 10–20 μm.

We have shown that the direct X-ray detection system using CCDs designed for optical detection functions well at several keV [4]. For high-energy X-rays of above several keV, the detection efficiency of this system depends on the thickness of the depletion region of the CCD. For low-energy X-rays of below 1 keV, on the other hand, the efficiency depends on the thickness of the structure above the depletion region. The optical CCDs usually have a depletion region made of silicon of about several μm in thickness and a surface layer of 1–2 μm in thickness made mainly of silicon dioxide above the depletion region. The mean absorption length in silicon is about 100 μm for 10 keV X-rays while that is only about 0.5 μm for 0.5 keV X-rays. Several groups [5, 6] are developing CCDs with a thick depletion region (~100 μm) in order to improve the detection efficiency at the high-energy region. In order to improve the detection efficiency below ~1 keV, however, we have to reduce the thickness of the front surface structure above the depletion

region. Another approach for soft X-ray detection is to use a back-side illumination type CCD [7] which functions well in this energy region since there is no gate structure in the backside.

In order to increase the sensitivity of the front-side illumination type CCD for soft X-rays, we have improved a virtual-phase CCD in cooperation with TI Japan Inc., which we call hereafter model TC223-S. The virtual-phase CCD [8] has the advantage that one half area of each pixel has no gate structure (virtual-phase) while the other half (gate-phase) has a standard gate structure. Therefore, the virtual-phase can be made sensitive to low-energy X-rays, if we can reduce the thickness of the protection structure above the depletion region. Since TC223-S has a protection layer of only 0.2 μm thickness, the detection efficiency of this CCD is expected to be approximately 1% even in the low-energy range of around 50 eV.

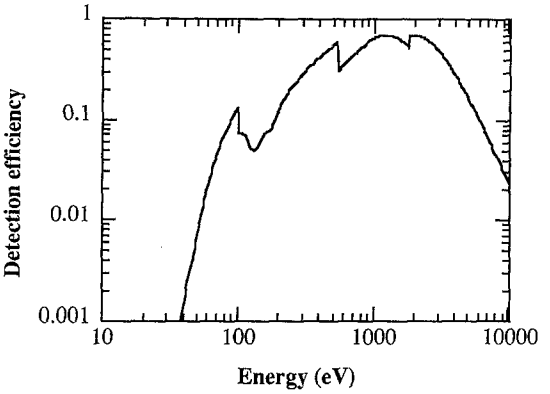

Fig. 1. Detection efficiency vs photon energy of a virtual-phase CCD with a thinned surface layer of 0.2 μm thickness

1 Experimental

1.1 Soft X-Ray CCD Camera

The CCD we have used is a newly developed frame transfer type CCD, TC223-S [9]. It contains 1024 × 1024 pixels each of which is a sqare of 18 μm × 18 μm. It is a virtual-phase CCD with thinned protection structure above the depletion region in order to improve the detection efficiency in the low photon energy of around several tens eV. The number of the electrons generated in the depletion region and stored in the charge storage channel is proportional to the number of the incident photons up to the saturation level which is about 5×10^5 electrons/pixel for this chip. The driver system and the data acquisition system are similar to those described previously [4]. All the digitized data are stored in a micro-computer. The CCD chip was placed onto a cold plate which was Peltier-cooled down to −50° C to reduce the thermal noise. The cold plate could be rotated in order to orient the CCD in a proper direction.

The exposure time, during which the CCD is in the integration mode, was programmed to be 10 s in this experiment. The integration was started manually and the X-ray laser pulse having a duration of approximately 0.5 ns was emitted within the exposure time. After exposure, all the charges were read out with a low-noise analogue electronics which was designed to saturate at the level of about 2×10^5 electrons/pixel (40% of the saturation level of the CCD chip). Each datum was converted to 12-bit digital datum. Background data were obtained before and after the exposure to remove the systematic error.

We have calibrated the absolute sensitivity of the TC223-S over the photon energies of 100–1000 eV with synchrotron radiation [9]. The measured sensitivities fit well with the calculated detection efficiencies for a CCD having a protection layer of 0.2 μm thickness, which is shown over 10–10000 eV in Fig. 1. Here the detection efficiency is defined as the fraction of the incident photons absorbed in the depletion region of the CCD. This result shows that the protection layer thickness of the TC223-S is estimated to be approximately 0.2 μm and the detection efficiency at around 50 eV is expected to be approximately 1%.

1.2 X-Ray Laser System

The experimental conditions are similar to the ones reported previously [10]. The laser medium was germanium which was evaporated in a stripe shape on a glass plate. The Ge stripe of 200 μm width and 1 μm thickness with a length of up to 5 cm was irradiated with a laser pulse of 1.053 μm wavelength, 1 ns duration and 1.1 kJ energy, which was focused onto the target to a line of 100 μm average width and 6 cm length. The average irradiance was 1.7×10^{13} W/cm^2. Five spectral lines belonging to $3p$–$3s$ transitions in neon-like Ge at the wavelengths of 196, 232, 236, 247, and 286 Å were amplified in the Ge plasma and emitted as an intense collimated radiation along the plasma axis. The direction of the X-ray laser beam was slightly off the target surface due to refraction in the plasma having a density gradient. A high resolution grazing incidence XUV spectrometer (Hettrick Scientific, Model HIREFS 170.5-25) [10], placed at approximately 9 mrad off the plasma axis, was used to measure the spectra. A horizontally-oriented spectrometer slit of 15 μm width was placed horizontally at 10 cm from the plasma center. With the combination of a grazing incidence spherical reflector and a varied-space planar grating, the spectrum was focused on a flat field perpendicular to the optical axis. A grazing incidence vertical reflector placed behind the grating weakly focused the horizontally diverging radiation in order to increase the flux on the detector. The spectrometer had a total optical distance from the slit to the detector plane of 5.6 m, with a dispersion at the detector of 0.886 Å/mm at 234 Å. Although we have not yet directly measured the resolution, it is expected, due to the careful alignment procedures we have taken in this experiment to satisfy the required accuracies, that the spectrometer had a resolving power close to the design value of 16000 at this wavelength.

The CCD was placed at the imaging plane of the spectrometer which was evacuated to 10^{-5} Torr with an auxiliary vacuum pump. Due to the small acceptance angle and proper aperturing in the spectrometer, optical stray light did not contribute to the observed spectra without using an optical blocking filter. When the X-ray laser intensity was too strong to saturate the detector, approximately one-third of the area containing the horizontally elongated spectral lines was covered with an aluminum filter of 0.5 μm thickness (measured

transmittance of 22%) in order to increase the dynamic range during recording. The sensitivity of the CCD was compared with a Kodak 101-07 film and an Ilford Q-plate whose sensitivities are approximately known from previous works.

2 Results and Analysis

2.1 General Scope of the CCD Image

We have recorded spectra of the X-ray laser beam under various experimental conditions. Figure 2 shows an example of the spectrum that was obtained using a slab target of 5 cm length. In obtaining these data, the CCD frame was tilted by $-3.5°$ with respect to the dispersion direction (horizontal direction in this figure) in order to avoid exact overlap of the narrow spectral lines with the pixel arrays. The length of the spectral lines normal to the dispersion direction is approximately 4 mm. The CCD chip is 18.4 mm × 18.4 mm that covers the wavelength region of approximately 16 Å. The spectral dispersion of 0.886 Å/mm and the pixel size of 18 μm gives a resolution of 15.9 mÅ/pixel.

These data were obtained without using any filter to record weak lines and thereby to test the sensitivity. The figure also shows two strong lasing lines and many weak spontaneous emission lines. The lasing lines due to $3p$–$3s$, $J = 2$–1 transitions in Ne-like Ge ions at the wavelengths of 236.26 Å and 232.24 Å are saturated not by the CCD chip but by the analogue electronics.

The spectrum obtained with the CCD was integrated over 36 μm (2 pixels) along the dispersion direction and over 2.88 mm (160 pixels) perpendicular to the dispersion direction, in which the tilt of the spectral lines relative to the pixel orientation was taken into account. The result is shown in Fig. 3. There are more than 20 lines seen in this figure whose approximate wavelengths and relative intensities are summarized in Table 1. The intensities of the two lasing lines are over 1000 times stronger than non-lasing lines. We notice a gradual increase in the continuum level toward a shorter wavelength. Detailed analyses and physical interpretations of the observed spectra will be reported elsewhere.

In the intensity scale that we use in this paper, one intensity unit corresponds approximately to 50 electrons per pixel. The read-out noise in this system, including the dark current, is about 1 intensity unit. Due to integration and

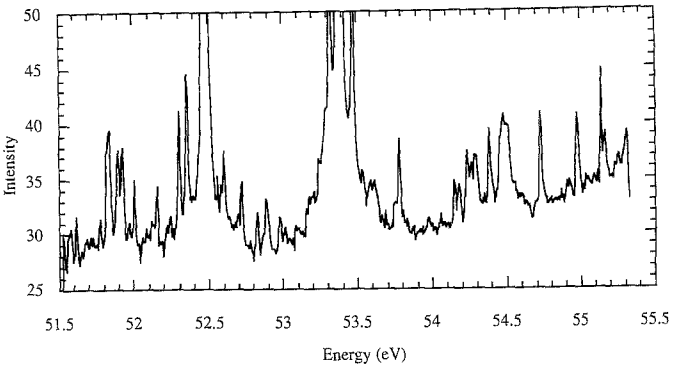

Fig. 3. The intensity profile along the dispersion direction in Fig. 2. Two strong lines around 52.5 eV (236 Å) and 53.4 eV (232 Å) are saturated due to the electronics used. Their predicted peak values in intensity are around 10000 in this scale

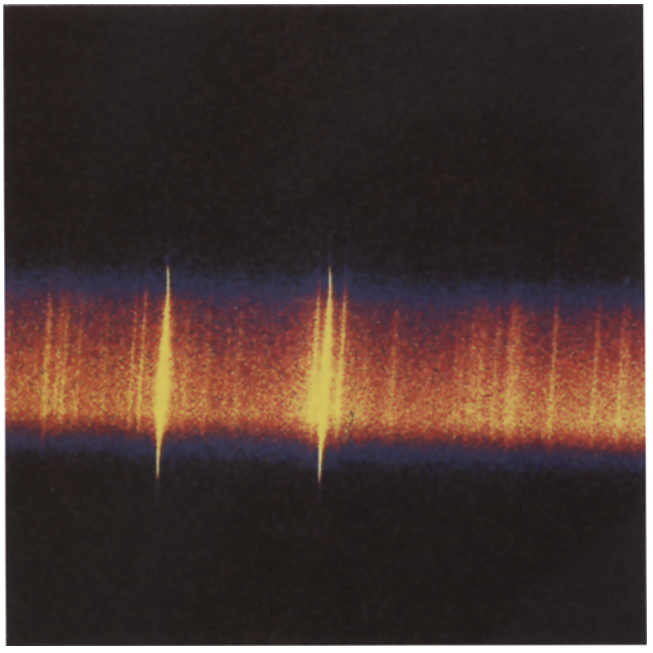

Fig. 2. A CCD image of the spectrum of the Ne-like Ge laser. The dispersion direction is horizontal in this figure with higher photon energy toward the right-hand side. Superposed on the weak continuum emission, more than 20 emission lines are observed, with two intense lasing lines at 236 Å and 232 Å. The colour coding is chosen to visually enhance the weak lines, making the lasing lines look completely saturated

Table 1. Emission lines observed in Fig. 2

Energy [eV]	Wavelength [Å]	Relative intensity	Transition
51.83	239.2	10	
51.90	238.9	8	
51.93	238.8	8	
52.01	238.4	6	
52.15	237.7	5	
52.30	237.1	10	
52.36	236.8	12	
52.48	236.3	~10000	Ge XXIII, $3p$–$3s$, $J = 2$–1
52.60	235.7	6	
52.72	235.2	5	
52.83	234.7	4	
52.89	234.4	5	
53.32	232.5	13	
53.39	232.2	~10000	Ge XXIII, $3p$–$3s$, $J = 2$–1
53.47	231.9	17	
53.78	230.5	8	
54.14	229.0	4	
54.18	228.8	4	
54.24	228.6	6	
54.26	228.5	4	
54.29	228.4	5	
54.38	228.0	7	
54.73	226.5	8	
54.98	225.5	7	
55.13	224.9	9	

averaging of the spectral signals over 320 pixels, the signal resolution improves by 18 times, i.e. it is 0.055 intensity unit, or 3 electrons per pixel. Since the saturation level is 4000 intensity units, the dynamic range exceeds 10000 and the response is linear over this range. This should be compared with the microchannel plates whose dynamic range is typically 1000. The Kodak 101 film, which has been used in various experiments in the soft X-ray region due to its high sensitivity ($\sim$1 photon/μm^2) and a relatively high spatial resolution ($\sim$5 μm), has a linear response range of $\sim$ 10 [11, 12].

The approximate sensitivity of this CCD could be evaluated alternatively by comparing the spectra such as the one shown in Fig. 2 with the spectra recorded with the X-ray films under the same experimental conditions. Many non-lasing lines that have been clearly recorded with the CCD shown in Figs. 2 and 3 were not observable with an Ilford Q-plate, whose sensitivity at this energy range is $\sim$1/3 of the Kodak 101 film, according to our calibration. With the Kodak 101-07 film, some of the stronger non-lasing lines were weakly visible with the optical densities of $\sim$0.2. Using the calibrated sensitivity of the 101 film at 160 Å [13], the photon flux required for exposure of O.D. $\sim$0.2 is evaluated to be approximately 4 photons/μm^2, corresponding to a flux of $\sim$1300 photons per CCD pixel of 18 μm $\times$ 18 μm, of which 50% is absorbed in the electrode covering half the area of each pixel. Assuming a 1% transmittance at the surface layer of the CCD to the 53.5 eV (232 Å) photon and considering that each 53.5 eV photon incident in the depletion layer will create 53.5 eV/3.65 eV = 15 electrons, where 3.65 eV is the ionization energy of Si, 650 photons will create 100 electrons in each pixel, or 2 intensity units. This value is consistent with the observed intensity with the CCD. Considering that the signal resolution of the CCD is 0.055 intensity units, we find that the CCD used in this experiment is slightly more sensitive than the Kodak 101 film even in this low-energy region, in addition to its superior linearity and a larger dynamic range.

2.2 Line Profile on the CCD

The energy resolution of this spectral image seems to be limited by the pixel size. However, we will show that we can calculate the line broadening with a precision better than that limited by the pixel size assuming that the data contain only one-dimensional information. This is possible because, due to the slight tilt of the CCD pixel relative to the spectral line, the line shape is scanned effectively by a detector which has a well-defined rectangular response function.

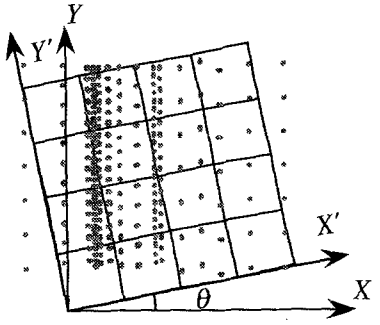

Fig. 4. A schematic view of a one dimensional spectral image on the CCD which is tilted by θ relative to the dispersion direction. Each data point of the CCD output is the integration over each pixel

We define the dispersion direction as the X-axis and assume that the CCD frame is tilted by an angle θ as shown schematically in Fig. 4. Each CCD datum represents an integration over each square shown in Fig. 4. Therefore, the output F_n of the pixel n can be described as

$$F_n = \int S(X) P_n(x,y)\,dx\,dy = \int S(x)\left[\int P_n(x,y)\,dy\right]dx\,, \tag{1}$$

$$P_n(x,y) = \begin{cases} \textit{Detection efficiency} & \text{over the pixel area } n\,, \\ 0 & \text{otherwise}\,, \end{cases}$$

where $S(x)$ is the line shape function of the incident flux. Since all the pixels on the CCD have an identical pixel size and shape with the same response $P_0(x,y)$ and their relative locations are well defined, we obtain the following equation,

$$\int P_n(x,y)\,dy = \int P_0[x-(x'\cos\theta - y'\sin\theta), y-(y'\cos\theta + x'\sin\theta)]\,dy = \mathrm{PSF}[x-(x'\cos\theta - y'\sin\theta)]\,, \tag{2}$$

where (x',y') is the CCD frame coordinate of the pixel n and PSF(x) is the point spread function (PSF) in the spectral analysis. Since $(x'\cos\theta - y'\sin\theta)$ is the x-coordinate of the pixel n, F_n can be expressed as a convolution by

$$F_n(x^0) = \int S(x)\mathrm{PSF}(x-x^0)\,dx\,, \tag{3}$$

where x^0 is the x-coordinate of the pixel n. Furthermore, x^0 can take various values depending on θ although (x',y') takes only discrete values. Therefore, we can expect that F_n will be almost continuous along the x coordinate.

From (3), we obtain

$$\sigma^2(F_n) = \sigma^2(S) + \sigma^2(\mathrm{PSF})\,, \tag{4}$$

where $\sigma(F)$ denotes the standard deviation of the function F, which is defined as $\exp(-x^2/2\sigma^2)$ for a Gaussian function. Since PSF is a function of the CCD pixel size as well as of θ, we obtain

$$\sigma^2(\mathrm{PSF}) = [(a\cos\theta)^2 + (b\sin\theta)^2]/12, \tag{5}$$

where a and b are the pixel sizes along the x' and y' coordinates, respectively. In our CCD, only the virtual phase is sensitive at the energy range we are concerned with. Since the direction of the virtual phase was horizontally oriented in this experiment, we take a and b as 18 μm and 9 μm, respectively. Furthermore, we assume that the detection efficiency is uniform over the virtual phase. Since σ(PSF) is determined exactly for the CCD using (5), $\sigma(S)$ can be determined better than the pixel size. The accuracy of $\sigma(S)$ depends on the accuracy of $\sigma(F_n)$.

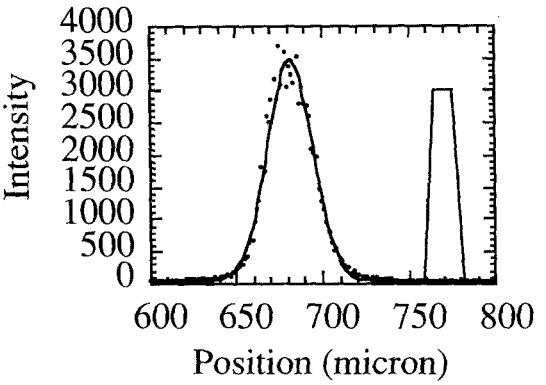

Fig. 5. Detailed line profile of the lasing line at 52.5 eV (236 Å). Dots are data points and the curve is the best Gaussian-function fit. The line profile is a convolution of the line shape function with the point spread function (PSF) of the CCD which is shown by the trapezoidal form in this figure

2.3 Data Analayis

In order to determine θ, which we do not know exactly, we have integrated the data along the Y-axis and obtained the one-dimensional data F_n along the X-axis for various angles θ. Assuming that the spectral data have only one-dimensional information, the line profile of F_n will be the narrowest at some value of θ, which we take as the true tilt angle. Figure 5 shows the line profile F_n for the 236 Å (52.5 eV) line recorded with a 4 cm long slab target. Due to proper filtering to attenuate the spectral intensities, the recorded lines are not saturated. The solid curve is the best fit to a Gaussian function whose parameters are summarized in Table 2. The trapezoidal shape in Fig. 5 is the PSF for these data. There is a slight deviation from the single Gaussian profile at the wing of the line profile. This example demonstrates the capability of the CCD for detailed spectral analyses.

In this analysis, we found that the observed width of the lasing line is broader than that of PSF which is $\sigma(\mathrm{PSF}) = 5.19\,\mu\mathrm{m}$. The expected width of the incident line $\sigma(S)$ calculated using (4) is shown in Table 2. The spectral width at full width at half maximum (FWHM) $\mathrm{d}\lambda$ is 25.3 mÅ for the 236 Å line. This width corresponds to the relative spectral width of approximately $\lambda/\mathrm{d}\lambda = 1 \times 10^4$. Considering the spectrometer resolving power of 16000 and assuming a Gaussian spectrometer response function, the intrinsic width of the 236 Å line is evaluated to be 20.5 mÅ. This 20.5 mÅ line width should be compared with the recent calculation [14] which gives a zero gain width for the 236 Å line to be 75 mÅ which gain-narrows to ~24 mÅ for the gain-length product of ~10 valid for these data. More detailed evaluation of the spectral widths will be reported elsewhere.

3 Discussion

We showed that the CCD can attain the spatial resolution better than the pixel size for one-dimensional data. Since the PSF is a fixed function, the spatial resolution can be evaluated from (4) as follows;

$$\sigma(F_n)\,\Delta\sigma(F_n) = \sigma(S)\,\Delta\sigma(S)\,. \tag{6}$$

In an exreme condition where $\sigma(S) \ll \sigma(\mathrm{PSF})$, we obtain the following relation,

$$\Delta\sigma(S) = [\sigma(\mathrm{PSF})/\sigma(S)]\,\Delta\sigma(F_n)\,. \tag{7}$$

If we define the ultimate spatial resolution $\Delta\sigma_{\mathrm{ult}}$ as $\sigma(S) = \Delta\sigma_{\mathrm{ult}}(S)$, it can be expressed as

$$\Delta\sigma_{\mathrm{ult}} = [\sigma(\mathrm{PSF})\,\Delta\sigma(F_n)]^{1/2}\,. \tag{8}$$

The value of $\Delta\sigma(F_n)$ depends on the signal-to-noise ratio of the data. The noise level is evaluated from the data in the area where no X-ray is detected. The uncertainty in $\sigma(F_n)$ is then calculated with the $\chi 2$ method based on the noise level mentioned before. In this way, $\Delta\sigma(F_n)$ is estimated to be about 0.2 μm in our experiment. Therefore, $\Delta\sigma_{\mathrm{ult}}$ in our CCD system can be as small as about 1 μm. If we take the FWHM as the linewidth resolving power, it is about 2 μm (about 1/10 of the pixel size). We should note that the uncertainty of the linewidth depends on the intrinsic linewidth.

In our analysis, we have assumed that the spectral data contain only one-dimensional information. In practice, the data show an intensity variation perpendicular to the dispersion direction. We restricted the spectral length to about 160 pixels over which there was an intensity variation of about 20%. Each datum point in Fig. 4 is the average of about 16 pixels. If the data are scattered more uniformly along the Y-axis, it will surely smooth out the intensity variation perpendicular to the dispersion direction. The line profiles shown in Fig. 5 do not seem to show a simple convolution

Table 2. Parameters for the 236 Å laser line

Transition	$(2p_{1/2}2p^4_{3/2}3p_{3/2})_{J=2}$–$(2p_{1/2}2p^4_{3/2}3s)_{J=1}$
Wavelength	236.26 Å
Width of the observed lineshape: σ	13.2 ± 0.2 μm
Width after subtraction of CCD PSF: $\sigma(S)$	12.1 ± 0.2 μm
: FWHM width[a]	28.5 ± 0.4 μm
	25.3 ± 0.4 mÅ
Width after subtraction of spectrometer response[b]	
: FWHM width	20.5 mÅ

[a] Assuming a Gaussian function, (FWHM width) $= 2.355 \times \sigma$

[b] Linewidth derived from [(linewidth)^2 – (spectrometer instrumental width)^2]$^{1/2}$, where the instrumental width was estimated from the resolving power of 16000 giving 14.8 mÅ. We have assumed that the spectrometer response function is given by a Gaussian function. If this function is given by a different function, the laser linewidth will become slightly (~1 mÅ) larger

expressed in (3). The data points scattered more than we expected probably partly due to the reason described before.

We have assumed that the X′ and Y′ coordinates of the pixels can be properly determined. In our analysis explained in Sect. 2.3, we have determined the tilt angle between the two coordinates by minimizing the linewidth. The uncertainty through this process, which depends on various factors such as the line shape, the spectral width and the signal to noise ratio, is about 0.05° in our data.

The line resolving power we have obtained can be understood as the best value from the practical point of view. Since the line intensities in Fig. 5 are almost saturated on the CCD, we cannot improve the signal to noise ratio. We can reduce $\Delta\sigma(F_n)$ by expanding the length of the spectrum up to the CCD chip size, improving the line resolving power by a factor of 2. However, the line shape will be distorted from the straight line, causing difficulties in the data analyses.

4 Conclusion

We have applied a newly developed CCD (TC223-S) that has a thinned protection layer (SiO_2) on the chip of approximately 0.2 μm to a soft X-ray laser experiment. The expected detection efficiency of this chip at around 50 eV is about 1%. This efficiency at 50 eV is several orders of magnitude higher than that of conventional CCD chips which have protection layers (SiO_2) of about 1–2 μm thickness. We have shown that the sensitivy of this CCD is slightly higher than a Kodak 101 film even at this low X-ray energy.

The spatial resolution of this direct X-ray detection system depends only on the pixel size of the CCD chip. In the case of indirect X-ray detection systems, in comparison, the line shape will be distorted to some extent due to the use of conversion instruments from the X-rays to the visible photons like the phosphor plate.

One of the advantages of the CCD is that the relative location of each pixel is well-known. This enables us to improve the line-resolving power since the apparent line shape can be expressed as a convolution between the intrinsic line shape and the pixel function. We have shown that the line resolving power can be improved to about 1/10 of the pixel size.

Acknowledgements. The authors express their thanks to D. Neely and A. MacPhee of Queens University of Belfast, the staffs at the Institute of Laser Engineering, and the CCD team member at the Faculty of Science, Osaka University for collaboration in this experiment. They also express their thanks to Mr. I. Fujii of TI Japan Inc. who gave us the technical support on the CCD used in this experiment. This work was partly supported by the Special Coordination Fund of the Science and Technology Agency.

References

1. E.E. Fill (ed.): *X-ray Lasers 1992*, Inst. Phys. Conf. Ser. No. 125 (Inst. Phys. Pub., Bristol 1992)
2. B.J. MacGowan, L.B. Da Silva, D.J. Fields, C.J. Keane, J.A. Koch, R.A. London, D.L. Matthews, S. Maxon, S. Mrowka, A.L. Osterheld, J.H. Scofield, G. Shimkaveg, J.E. Trebes, R.S. Walling: Phys. Fluids B **4**, 2326 (1992)
3. H. Tsunemi, M. Wada, K. Hayashida, S. Kawai: Jpn. J. Appl. Phys. **30**, 3540 (1991)
4. H. Tsunemi, S. Kawai, K. Hayashida: Jpn. J. Appl. Phys. **30**, 1299 (1991)
5. B.E. Burke, R.W. Mountain, D.C. Harrison, M.W. Bautz, J.P. Doty, G.R. Ricker, P.J. Daniels: IEEE Trans. ED-**38**, 1069 (1991)
6. L. Strüder, H. Bräuninger, M. Meier, P. Predehl, C. Reppin, M. Sterzik, J. Trümper, P. Cattaneo, D. Hauff, G. Lutz, K. F. Schuster, A. Schwarz, E. Kenziorra, A. Staubert, E. Gatti, A. Longoni, M. Sampietro, V. Radeka, P. Rehak, S. Rescia, P. F. Manfredi, W. Buttler, P. Holl, J. Kemmer, U. Prechtel, T. Ziemann: Nucl. Instrum. Methods A **288**, 227 (1990)
7. C. Castelli, A. Wells, K. McCarthy, A. Holland: Nucl. Instrum. Methods A **310**, 240 (1991)
8. J. Hynecek: IEDM Tech. Digest **78** (1979)
9. S. Nomoto: Master Thesis, Osaka University (1993)
10. Y. Kato, H. Daido, H. Shiraga, M. Yamanaka, H. Azuma, K. Murai, E. Miura, G. Yuan, M. Ohmi, K. Tanaka, T. Kanabe, M. Takagi, S. Nakai, C.L.S. Lewis, D.M. O'Neill, D. Neely, K. Shinohara, M. Niibe, Y. Fukuda: Proc. SPIE **1551**, 56 (1991)
11. B.L. Henke, S.L. Kwok, J.Y. Uejio, H.T. Yamada, G.C. Young: J. Opt. Soc. Am. B **1**, 818 (1984)
12. B.L. Henke, F.G. Fujiwara, M.A. Tester, C.H. Dittmore, M.A. Palmer: J. Opt. Soc. Am. B **1**, 828 (1984)
13. K. Eidmann, T. Kishimoto, P. Herrmann, J. Mizui, R. Pakula, R. Sigel, S. Witkowski: Laser Part. Beams **4**, 521 (1986)
14. P.B. Holden, S.B. Healy, M.T.M. Lightbody, G.J. Pert, A. Kingston, E. Robertson, C.L.S. Lewis, D. Neely: J. Phys. B, to be published